(18) Lin, J.; Tsuji, K.; Williams, Ff. *Trans. Faraday Soc.* **1968**, *64*, 2896.
(19) Schneider, C.; Swallow, A. J. *Makromol. Chem.* **1968**, *114*, 155.
(20) The rection of the dimer radical cations with methanol has been reported to form 1,4-dimethyl-1-methoxy-1,4-diphenylbutane. See: Asanuma, T.; Gotoh, T.; Tsuchida, A.; Yamamoto, M.; Nishijima, Y. *J. Chem. Soc., Chem. Commun.* **1977**, 485.

Spherical Macroions in Strong Fields†

Marshall Fixman* and Salem Jagannathan‡

Department of Chemistry, Colorado State University, Fort Collins, Colorado 80523.
Received September 7, 1982

ABSTRACT: The steady-state response of a dilute salt solution of spherical macroions to strong electrical fields has been calculated on the basis of the nonlinear diffusion equations, the Navier–Stokes equation, and Poisson's equation. The electrophoretic mobility shows essentially no nonlinear response at the field strengths considered, but the effective charge and dipole moment, the latter proportional to the conductivity change, show a strongly nonlinear response. At moderate field strengths part of the ion atmosphere is stripped away, but at still larger fields the macroion traps counterions. A positively charged macroion together with its ion atmosphere then has a net negative charge. If the Debye length κ^{-1} and radius a are such that $\kappa a > 1$, as holds for the numerical illustrations, nonlinearity in the polarization or nonquadratic response of the effective charge sets in at field strengths that scale inversely with particle radius. The field strength can therefore be quite low compared to what is required for Wien effects in strong electrolyte solutions, where the required field scales as κ.

I. Introduction

A considerable amount of experimental and theoretical work has been done on nonlinear phenomena in simple electrolytes, especially concerning the Wien effects[1] (increasing conductivity with field strength). No comparable body of theory, or experiments designed to advance theory, seems to exist for macroions or polyelectrolytes. Strong electrical fields are often used for the orientation of anisotropic macroions, and it is sometimes found that molecules not believed to have a permanent moment behave as if they did.[2] So it may be that the polarization of the ion atmosphere is exhibiting a saturation. The main motivation for this work is the exploration of nonlinear effects in the polarization of the ion atmosphere. Incidental results are gathered on the electrophoretic velocity, on the apparent charge that arises from destruction of the ion atmosphere, and on the complex conductivity.

The problem is somewhat more difficult than the corresponding one for simple electrolytes. The electrostatic potentials are usually large compared to k_BT and essentially nothing can be linearized. Electrophoretic effects and convective transport of salt ions are large, and the Navier–Stokes equation is fully coupled with the diffusion equations for the salt ions. It has therefore seemed sensible to start the work with spheres rather than with anisotropic bodies, for which interesting experiments may be easier.

Except for one generalization of great interest but uncertain merit, our basic equations are those used for electrophoresis by Overbeek et al.[3] However, we have followed the notation and formulation of our previous work.[4] Advances in computers and numerical analysis have now brought those equations to the point of fairly routine solubility for linear problems involving spheres. See the work of O'Brien and White[5] on electrophoresis and DeLacey and White[6] on the complex conductivity. Nonlinear problems and the study of anisotropic bodies[7–9] have not yet reached that stage.

† Supported in part by NIH GM27945.
‡ Present address: Department of Chemistry, Princeton University, Princeton, NJ.

The generalization we mentioned consists in allowance for a coefficient of sliding friction at the surface of the macroion. The velocity gradients near the surface of a macroion can be quite enormous by usual standards. Due to the force exerted on high charge densities by the applied electric field, the solvent is accelerated to the electrophoretic velocity over distances comparable to the Debye length. This length may of course be much smaller than the dimensions of the macroion, which would ordinarily characterize the length scale. Consequently one anticipates that the usual sticking boundary condition may be inadequate. (The suggestion has been made that electrophoretic mobilities may show nonlinear effects originating in breakup of the boundary layer at a few volts/cm.[10] Some scepticism may be warranted in regard to the explanation, but the observation is intriguing.) Our intent here is limited to a comparison between the effects of slippage on a macroion in an electric field, and the sedimentation of an uncharged object. The nature and characterization of slippage between a liquid and solid boundary have received some attention for simple systems,[11] but none that we know of for electrolyte solutions.

In outline our work is as follows. In section II the basic equations are reviewed. The only novelty here is the use of the Stokes "stream function", which considerably simplifies problems of "axisymmetric" flow.[12] There is no special advantage to it for linear problems, and indeed it cannot be used for some interesting linear problems involving rotation or shear. However, this work is restricted to a constant vector applied field, either electrical or centrifugal (or both if they are parallel), of arbitrary amplitude. The symmetry is sufficient that the flow must remain axisymmetric no matter how large the applied force. A preliminary discussion of boundary conditions is given for the purpose of relating the quantities of direct physical interest to the asymptotic behavior of the solutions. The quantities of direct physical interest are assumed to be restricted to the electrophoretic velocity, the apparent dipole moment, and perhaps the apparent charge of the macroion system. The dipole determines the conductivity increment. The theory is confined in all respects

0024-9297/83/2216-0685$01.50/0

to dilute solutions, and only a single macroion is considered.

In section III the asymptotic behavior of the various fields is considered, and also the boundary conditions on the surface of the sphere. The main purpose of the former considerations is to establish that the distorted charge density vanishes at infinity with sufficient rapidity that multipole expansions of the fields are justifiable in principle. Considerably more can be done to establish the asymptotic behavior for weak, oscillating fields.[6] We consider this problem only to a limited extent, sufficient to contrast the behavior in that case against the nonlinear steady-state behavior, and to provide a basis for tests of thin-layer theory reported in the following paper.[13] For the nonlinear problem we have had to use asymptotic fields that are rather crude in their account of the charge density. The main reason for this was the inability of the "shooting method", described in section VI, to deal with integrations across a large range of distance. Despite the fact that numerical integrations were started at about 15 Debye lengths from the macroion surface, the fractional perturbations in concentration were by no means small at our larger applied field strengths.

In sections IV and V the field equations and boundary conditions are all expanded in appropriate polynomials in $\cos\theta$ (Legendre polynomials for the scalar potentials and Gegenbauer polynomials for the velocity potentials). The numerical approach is outlined in section VI, and a sketch of results is given in section VII.

It seems probable that pulse techniques could produce a body of useful information about the nonlinear response of macroions, that theoretical results could be tested, and that interesting information could be obtained about the flow of solvent near the macroion surface. We are not aware of any applicable data for spheres. So at the moment the main purpose served by this work is the generation of methodology and results which can help guide theoretical work on anisotropic bodies.

II. Basic Equations

The formulation presented previously[4] is here extended slightly. First, the linearization and approximations introduced for thin double layers, in section IIIC[4] and subsequently, are here abandoned. Throughout, arbitrarily large perturbations of the equilibrium system are permitted. Also, an external force is allowed in addition to, or in place of, the external electrical field $\mathbf{E}_0$. The new force is assumed to arise from a constant acceleration $\mathbf{g}$ applied to every element of mass in the system. The notation on the whole is that used previously, with one significant exception. The symbol $\mathbf{R}$, previously used to designate a position vector in the laboratory frame, will here designate the dimensionless position vector $\kappa\mathbf{r}$. As before, $\mathbf{r}$ is a position vector relative to the center of the macroion, and κ^{-1} is the Debye length.

A. Force Balance Equation. Equations for the solution velocity and electrical fields are summarized here. An initial connection is drawn between the asymptotic behavior of the two fields.

At any point $\mathbf{r}$, whether in the solution or in the macroion, the total force density would usually be set equal to the product of mass density $m(\mathbf{r})$ and the acceleration of a mass element at $\mathbf{r}$. Here we neglect this inertial force, on the grounds previously stated,[4] and put

$$\nabla_r\cdot\sigma + [m(\mathbf{r}) - m_S]\mathbf{g} = 0 \tag{2.1}$$

where m_S is the mass density of the solution and σ is the sum of viscoelastic and electrical stresses. A term $m_S\mathbf{g}$ has been explicitly subtracted from the external force density in eq 2.1, and this has been compensated by an equivalent (implicit) subtraction from the pressure gradient in $\nabla_r\cdot\sigma$. With these subtractions the stress tensor vanishes (or at least reduces to a constant pressure) at infinity. Integration of eq 2.1 over a sphere of radius B centered on the macroion gives

$$\mathbf{F} + (m_M - m_S)\mathbf{g}V_M = 0 \tag{2.2}$$

where V_M is the volume of the macroion and m_M is its mass density. $\mathbf{F}$ is the volume or surface integral

$$\mathbf{F} \equiv \int_B \nabla_r\cdot\sigma \, d\mathbf{r} = B^2\int_B \sigma\cdot\mathbf{e}_r \, de_r \tag{2.3}$$

The surface at B lies in the solution phase, near the macroion, and an explicit expression for σ may be confined to that phase. It may be shown[4] that the value of $\mathbf{F}$ is independent of B. We therefore take $B \to \infty$ and evaluate $\mathbf{F}$ from asymptotic solutions.

In the solution σ is the sum of the viscous and electrical stresses, $\sigma = \sigma^H + \sigma^E$.

$$\sigma^H = 2\eta(\nabla_r\mathbf{v})^{sym} - P\mathbf{1}$$

$$\nabla_r\cdot\sigma^H = \eta\nabla_r^2\mathbf{v} - \nabla_r P \tag{2.4}$$

and

$$\sigma^E = (D/4\pi)[\mathbf{EE} - \tfrac{1}{2}E^2\mathbf{1}] \tag{2.5}$$

$$\nabla_r\cdot\sigma^E = \rho\mathbf{E}$$

respectively. $\mathbf{v}$ is the velocity, η is the shear viscosity, $\mathbf{E}$ is the electrical field, D is the solvent dielectric constant, and ρ is the charge density. These equations and eq 2.1 give the appropriate form of the Navier–Stokes equation, which is used outside the macroion.

$$\eta\nabla_r^2\mathbf{v} - \nabla_r P + \rho\mathbf{E} = 0 \tag{2.6}$$

The electrical field satisfies Poisson's equation,

$$\nabla_r\cdot[D(\mathbf{r})\mathbf{E}] = 4\pi\rho \tag{2.7}$$

$D(\mathbf{r})$ is allowed to have a discontinuity across the macroion surface. Equations 2.6 and 2.7 are the basic differential equations for $\mathbf{v}(\mathbf{r})$ outside the macroion and for $\mathbf{E}(\mathbf{r})$ everywhere.

For the calculation of $\mathbf{F}$ the leading terms in the asymptotic expansions of $\mathbf{v}$ and $\mathbf{E}$ are required. These expansions are naturally expressed in terms of the Green's functions for the respective equations, namely, $1/r$ for Poisson's equation and the Oseen tensor $\mathbf{T}(\mathbf{r})$ for the Navier–Stokes equation. It should be clear that the asymptotic fields displayed in this paragraph are not assumed to describe the actual fields inside or near the macroion. The differential equations everywhere satisfied by the asymptotic fields are introduced only to help evaluate the surface integral of eq 2.3.

$$\mathbf{v}(\mathbf{r}) \sim -\mathbf{V}^0 - \mathbf{T}(\mathbf{r})\cdot\mathbf{F}^H + \ldots \tag{2.8}$$

where

$$\mathbf{T}(\mathbf{r}) \equiv (\mathbf{1} + \mathbf{e}_r\mathbf{e}_r)/(8\pi\eta r)$$

$$P \sim -(\mathbf{F}^H\cdot\nabla_r r^{-1})/4\pi + \ldots \tag{2.9}$$

The constant vector $\mathbf{V}^0$ is the drift velocity of the macroion in whatever applied fields are present. $\mathbf{F}^H$ is the apparent hydrodynamic force on the macroion. The displayed terms of eq 2.8 satisfy

$$\nabla_r\cdot\sigma^H = \eta\nabla_r^2\mathbf{v} - \nabla_r P = \mathbf{F}^H\delta(\mathbf{r}) \tag{2.10}$$

and therefore

$$\int_B \nabla_r\cdot\sigma^H \, d\mathbf{r} = \mathbf{F}^H \tag{2.11}$$

The electrical field is obtained from

$$\mathbf{E} = \mathbf{E}^0 + D^{-1}[-q\nabla_r r^{-1} + (\nabla_r\nabla_r r^{-1})\cdot\mu + ...] \quad (2.12)$$

where q and μ are the apparent charge and dipole moment, respectively, of the macroion plus its (deformed) ion atmosphere. Through the monopole term of eq 2.12, $\mathbf{E}$ satisfies Poisson's equation

$$\nabla\cdot\mathbf{E} = 4\pi\rho/D \quad (2.13)$$

with

$$\rho = q\delta(\mathbf{r})$$

Therefore

$$\nabla_r\cdot\sigma^E = q\delta(\mathbf{r})[\mathbf{E}^0 + q\mathbf{e}_r/(Dr^2)] \quad (2.14)$$

and

$$\mathbf{F}^E \equiv \int_B \nabla_r\cdot\sigma^E \, d\mathbf{r} = q\mathbf{E}^0 \quad (2.15)$$

(A slightly broadened δ function can be used to eliminate the product of singularities in eq 2.14. The unit vector $\mathbf{e}_r$ remains to make the product vanish after angular integration.)

The force $\mathbf{F}$ is the sum, on the surface B, of its hydrodynamic and electrical parts, $\mathbf{F}^H$ and $\mathbf{F}^E$, respectively, and eq 2.2 becomes

$$\mathbf{F}^H + q\mathbf{E}^0 + \mathbf{F}^g = 0 \quad (2.16)$$

where

$$\mathbf{F}^g \equiv (m_M - m_S)\mathbf{g}V_M$$

This equation serves to determine the asymptotic velocity parameter $\mathbf{F}^H$ in terms of the applied fields and the apparent charge q. For small applied fields q is proportional to the square of the applied field and may be suppressed in a theory restricted to linear response. (That q does not depend linearly on the applied fields can be taken as obvious on symmetry grounds, since q is a scalar and the applied fields are vectors.) Here q must be retained.

B. Diffusion and Electrochemical Potentials. The mobile salt ions, labeled $i = 1, ..., I$, are presumed to satisfy the force balance equation

$$-\beta_i(\mathbf{v}_i - \mathbf{v}) - k_BT\nabla_r \ln C_i + q_i\mathbf{E} = 0 \quad (2.17)$$

where, for ion i, β_i is a friction constant, $\mathbf{v}_i$ the drift velocity, q_i the charge, and C_i the number density. This equation is supplemented by the conservation equation

$$\partial C_i/\partial t = -\nabla_r\cdot(C_i\mathbf{v}_i) \quad (2.18)$$

In practice we retain the time derivative only for weak, oscillating applied fields. In the notation used previously,[4] several useful potentials may be defined. A "chemical" potential h_i is defined in terms of the actual concentration C_i and the equilibrium concentration C_i^e by

$$h_i(\mathbf{r}) \equiv \ln [C_i(\mathbf{r})/C_i^e(\mathbf{r})] \quad (2.19)$$

The equilibrium concentration at $\mathbf{r}$ is related to the equilibrium electrostatic potential Ψ^e by the Poisson–Boltzmann expression implicit in eq 2.17,

$$C_i^e(\mathbf{r}) = \bar{C}_i \exp[-q_i\Psi^e/k_BT] \quad (2.20)$$

where $\bar{C}_i$ is the bulk concentration of ion i. With Φ defined by

$$\mathbf{E} \equiv -\nabla_r\Psi$$
$$\Psi \equiv \Psi^e + \Phi \quad (2.21)$$

the drift velocity is given by

$$\mathbf{v}_i = \mathbf{v} - D_i\nabla_r p_i \quad (2.22)$$

where

$$D_i \equiv k_BT/\beta_i \quad (2.23)$$

and p_i is an "electrochemical" potential

$$p_i = h_i + (q_i/k_BT)\Phi \quad (2.24)$$

Equations 2.18 to 2.20, eq 2.22, and the incompressibility of solvent give

$$D_i^{-1}(\partial h_i/\partial t) = (D_i^{-1}\mathbf{v} - \nabla_r p_i)\cdot\nabla_r[(q_i\Psi^e/k_BT) - h_i] + \nabla_r^2 p_i \quad (2.25)$$

This set of I equations is the basis of our calculation of the p_i (or h_i). It has to be supplemented by equations for the electrostatic potential and the velocity field.

The electrostatic potential is determined by Poisson's equation

$$\nabla_r\cdot[D(\mathbf{r})\nabla_r\Psi] = -4\pi[\rho + \rho_M\delta(r - a)] \quad (2.26)$$

where ρ_M is the surface charge density on the macroion, which is presumed to have radius a. ρ now stands for the charge density due to mobile ions. Outside the macroion ρ is given by

$$\rho = \sum C_iq_i \quad (2.27)$$

$$= \sum q_i\bar{C}_i \exp[h_i - q_i\Psi^e/k_BT] \quad (2.28)$$

The equilibrium potential Ψ^e is obtained by suppression of h_i in the last equation and may be characterized by its value or derivative at $r = a$.

$$\Psi^e(a) = \zeta \quad (2.29)$$

$$(\partial\Psi^e/\partial r)_a = -4\pi\rho_M/D \quad (2.30)$$

The first characterization, in terms of the "ζ potential", is conventional in electrophoretic theory.

Another potential, the Stokes stream function S,[12] is convenient in the treatment of the velocity field. The definition and fundamental properties of the stream function are presented below.

C. Stream Function. All applied fields are assumed to lie along the z axis of the laboratory and macroion coordinate systems. This is a superficial convenience in the linearized theory, where the response is additive over all applied fields and the direction of each of them is arbitrary. For the nonlinear problems a real restriction is imposed: if centrifugal and electrical applied fields are both present, they must lie along the same axis. The restriction is imposed to force a uniaxial symmetry on the system and thereby justify use of the Stokes stream function $S(r,\theta)$. Solvent and solution incompressibility is also required. The arguments required to establish the following equations are presented in Happel and Brenner,[12] except that the body force $\rho\mathbf{E}$ must now be included in the Navier–Stokes equation. (Their discussion is not easily contracted or summarized, so the main results are simply quoted. The only difference is that eq 2.34 below now has a source term on the right-hand side.)

In a spherical coordinate system (r,θ,φ) centered on the macroion, a function $S(r,\theta)$ exists independent of φ and such that

$$\mathbf{v} = (r \sin\theta)^{-1}\mathbf{e}_\varphi \times \nabla_r S(r,\theta) \quad (2.31)$$

The two nonvanishing components of $\mathbf{v}$ are

$$v_r = -(r^2 \sin\theta)^{-1}\partial S/\partial\theta \quad (2.32)$$

$$v_\theta = (r \sin\theta)^{-1}\partial S/\partial r \quad (2.33)$$

The equation satisfied by S is

$$\eta \mathcal{M}^2 S = \sin^2\theta \left[\frac{\partial \rho}{\partial c}\frac{\partial \Psi}{\partial r} - \frac{\partial \rho}{\partial r}\frac{\partial \Psi}{\partial c} \right] \tag{2.34}$$

where

$$c \equiv \cos\theta$$

and

$$\mathcal{M} \equiv \frac{\partial^2}{\partial r^2} + \frac{\sin^2\theta}{r^2}\frac{\partial^2}{\partial c^2} \tag{2.35}$$

D. Dimensionless Variables. The chemical and electrochemical potentials h_i and p_i have been defined as dimensionless variables. The coordinate vector, the electrical and velocity fields, and the differential equations for all quantities have still to be put in dimensionless form.

1. Electrical Field. Let

$$\psi \equiv e\Psi/k_BT$$
$$\phi \equiv e\Phi/k_BT \tag{2.36}$$

and

$$\mathbf{R} \equiv \kappa \mathbf{r} \tag{2.37}$$

where e is the proton charge. The dimensionless electrical field vector is

$$\mathcal{E} \equiv -\nabla_R \psi = e\mathbf{E}/(\kappa k_BT) \tag{2.38}$$

The magnitude of the dimensionless field is the potential drop across a Debye length, in units of k_BT.

In dealing with the mobile ion charge density, several auxiliary parameters are convenient. Let

$$q_i \equiv ez_i$$
$$p_i \equiv h_i + z_i\phi$$
$$\bar{C}_i = \nu_i \bar{C} \tag{2.39}$$

where z_i is the number of positive elementary charges carried by i, $\bar{C}$ is the concentration of "neutral salt molecules", and ν_i is the number of ions of species i supplied by each salt molecule. The definition of a neutral salt molecule is subject to the neutrality condition

$$\sum \nu_i z_i = 0 \tag{2.40}$$

but is otherwise arbitrary. The Debye–Hückel screening length κ^{-1} is defined by

$$\kappa^2 = (4\pi \bar{C} e^2/Dk_BT)\sum \nu_i z_i^2 \tag{2.41}$$

Introduction of the reduced potential and coordinates into Poisson's equation leads to a dimensionless measure $\tilde{\rho}$ of charge density related to ρ by

$$\rho(\mathbf{r}) = (k_BTD\kappa^2/4\pi e)\tilde{\rho}(\mathbf{r}) \tag{2.42}$$

where

$$\tilde{\rho} \equiv \sum Z_i \exp(h_i - z_i\psi^e) \tag{2.43}$$

and

$$Z_i \equiv \nu_i z_i / \sum \nu_j z_j^2 \tag{2.44}$$
$$\sum Z_j = 0 \qquad \sum z_j Z_j = 1$$

Poisson's equation for the solution phase then becomes

$$\nabla_R^2 \psi = -\tilde{\rho} \tag{2.45}$$

The dimensionless equilibrium potential ψ^e is again recovered from eq 2.43 and 2.45 with the h_i set to zero.

2. Diffusion Potentials. Equation 2.25 involves the velocity and time in addition to other variables previously put in dimensionless form. Define then the dimensionless measure of time

$$\tau = (k_BT\kappa^2/6\pi\eta\mathcal{B})t \tag{2.46}$$

and the dimensionless velocity $\mathbf{u}$

$$\mathbf{u} = (6\pi\eta\mathcal{B}/\kappa k_BT)\mathbf{v} \tag{2.47}$$

where $\mathcal{B}$ is the Bjerrum length

$$\mathcal{B} \equiv e^2/Dk_BT \tag{2.48}$$

Equation 2.25 becomes

$$\gamma_i \partial h_i/\partial\tau = (\gamma_i \mathbf{u} - \nabla_R p_i)\cdot\nabla_R(z_i\psi^e - h_i) + \nabla_R^2 p_i \tag{2.49}$$

where γ_i is defined in terms of a Stokes law radius a_i, $\beta_i = 6\pi\eta a_i$,

$$\gamma_i \equiv a_i/\mathcal{B} \tag{2.50}$$

3. Velocity Potential. In order to preserve the simple relation between velocity components and the stream function, a dimensionless stream function s is defined by

$$s \equiv (6\pi\eta\mathcal{B}\kappa/k_BT)S \tag{2.51}$$

Then

$$u_R = R^{-2}\partial s/\partial c \tag{2.52}$$

and

$$u_\theta = (R\sin\theta)^{-1}\partial s/\partial R \tag{2.53}$$

Equation 2.34 for the stream function becomes

$$\mathcal{N}^2 s = \frac{3}{2}\sin^2\theta\left(\frac{\partial \tilde{\rho}}{\partial c}\frac{\partial \psi}{\partial R} - \frac{\partial \tilde{\rho}}{\partial R}\frac{\partial \psi}{\partial c} \right) \tag{2.54}$$

where

$$\mathcal{N} \equiv \frac{\partial^2}{\partial R^2} + \frac{\sin^2\theta}{R^2}\frac{\partial^2}{\partial c^2} \tag{2.55}$$

An alternative expression for the source term in eq 2.54 follows from substitution of the identity

$$h_i = p_i - z_i(\psi - \psi^e) \tag{2.56}$$

in eq 2.43 for the reduced charge density.

$$\mathcal{N}^2 s = \frac{3}{2}\sin^2\theta \sum_i Z_i \exp(p_i - z_i\psi)\left[\frac{\partial p_i}{\partial c}\frac{\partial \psi}{\partial R} - \frac{\partial p_i}{\partial R}\frac{\partial \psi}{\partial c} \right] \tag{2.57}$$

Inspection of eq 2.57 shows that ψ may be replaced by ψ^e, and p_i suppressed in the expontential, if only the linear response is wanted. This is in accord with the observation of O'Brien and White[5] that the perturbation in electrostatic potential is not required in the linear electrophoretic theory of the sphere. However, this decoupling is not maintained in the nonlinear theory, in the study of oscillatory problems, or if more exotic boundary conditions on the surface velocity are allowed than we or they consider (see section IIIB).

III. Boundary Conditions

The main question taken up in this section is the asymptotic behavior of the fields at large distances from the macroion. The asymptotic behavior is important in two aspects, first with regard to the inference of physical properties, and second with regard to the numerical solution of the differential equations. Boundary conditions on the surface of the macroion are mathematically

straightforward. However, some physical questions do arise in connection with partial slip. These questions are considered at the end of this section.

Knowledge of asymptotic behavior is practically important in the numerical work. If this behavior is poorly known, the numerical integration has to be started at a distant outer boundary. And since the equations are somewhat unstable, long integration ranges are undesirable. Only a few properties of the asymptotic expansions have immediate physical relevance, as far as we know. These are the velocity at infinity, equivalent to the electrophoretic velocity, and the apparent dipole moment, which determines the (complex) conductivity or dielectric modulus. However, a great many other boundary conditions have to be specified to solve the equations.

The asymptotic equations that have to be considered are naturally quite similar to those for the Wien effect in simple electrolytes.[1] However, several complications are present that make the problem difficult relative to the classical work.[1] First, the equilibrium potential is not small and does not serve as an ordering parameter. Second, the differential equations do not apply everywhere, but only outside a finite macroion. Therefore sources of unknown strength have to be added to the differential equations, to permit the surface boundary conditions to be satisfied. Finally, the fields have sooner or later to be expanded in spherical harmonics to allow matching of the inner boundary conditions, whereas the asymptotic fields have a compact representation only in cylindrical coordinates.

For linear problems involving colloids or macroions, the asymptotic behavior has been fully discussed by White et al.[5,6] for both steady-state and oscillatory motion. We have retained in our equations the terms necessary for linear oscillatory motion. However, the methods used here were designed for the nonlinear steady-state problem and therefore bear more resemblance to the methods used for the Wien effect[1] than to those of DeLacey and White.[6] Because the asymptotic equations are quasi-linear, the differences are not major.

The study of asymptotic behavior centers on the concentration fields h_i. The concentrations determine the charge density, and from that the electrostatic field. The remaining field, the stream function, is found in practice to converge fairly rapidly to simple asymptotic behavior, and no special attention is given to it at this point. It is considered in section V, along with the spherical harmonic expansions of other fields.

In this section the study of boundary conditions is carried only to the point where a choice of coordinate representations has to be made for further progress.

A. Asymptotic Behavior of the h_i. Certain leading terms in the solution are known immediately. The h_i measure concentration perturbations and vanish at infinity. The electric field and velocity enter the equations for h_i. At infinity the electric field approaches a constant $\mathcal{E}^0$. The velocity $\mathbf{u}$ approaches a constant $-\mathbf{U}^0$, where $\mathbf{U}^0$ is the macroion velocity in dimensionless units. Equation 2.16 relates the next order terms in the asymptotic behavior of velocity and electric fields. The charge density also enters the equations for h_i. The charge density is determined in eq 2.43 by the h_i, or at large R by just the sum of Z_ih_i. So the asymptotic behavior of the h_i has to be studied in order to understand the charge decay.

At large R, ψ^e decays as e^{-R}/R and is presumed to be neglible in the region under consideration. Then eq 2.43 and 2.45 give

$$\begin{aligned}\nabla_R{}^2\phi &= -(\tilde{\rho} - \tilde{\rho}^e) \\ &= -[h + \tfrac{1}{2}\textstyle\sum Z_ih_i{}^2 + \ldots] \end{aligned} \tag{3.1}$$

where

$$\begin{aligned} h &\equiv \sum_{i=1}^{I} Z_ih_i \\ &\sim (\tilde{\rho} - \tilde{\rho}^e) \end{aligned} \tag{3.2}$$

The terms of order $h_i{}^2$ in eq 3.1 may be suppressed in the asymptotic expansion. However, as will be amplified in section V, it is doubtful whether the asymptotic region of the charge density was reached in practice.

Since $p_i = h_i + z_i\phi$, eq 2.49 can be written

$$\nabla_R{}^2h_j - z_jh + \mathbf{L}_j{}^0\cdot\nabla_Rh_j - \gamma_j\partial h_j/\partial\tau = t_j(\mathbf{R}) \tag{3.3}$$

where

$$\mathbf{L}_j{}^0 \equiv \gamma_j\mathbf{U}^0 - z_j\mathcal{E}^0 \tag{3.4}$$

and $t_j(\mathbf{R})$ is a source term. In principle, $t_j(\mathbf{R})$ represents the nonlinear terms that have been suppressed in eq 3.3, and the equation applies only outside the macroion. In practice, eq 3.3 is assumed to apply for all $\mathbf{R}$, but the solutions are used only for large R. $t_j(\mathbf{R})$ is inserted to generate asymptotic behavior and is a sum of δ functions and derivatives of δ functions with varying amplitudes. These amplitudes represent the parameters used to characterize the asymptotic behavior. The asymptotic solutions of (3.3) are wanted in two special cases: (1) linearized oscillatory motion with time dependence $\exp(i\omega\tau)$, and (2) steady-state nonlinear motion. These cases are treated simultaneously. Equation 3.3 may now be written

$$\nabla_R{}^2h_j - z_jh + \mathbf{L}_j{}^0\cdot\nabla_Rh_j - i\omega\gamma_jh_j = t_j(\mathbf{R}) \tag{3.5}$$

Equation 3.5 is soluble by Fourier transform techniques. Let

$$h_j(\mathbf{R}) = \int H_j(\mathbf{k})\,\exp(i\mathbf{k}\cdot\mathbf{R})\,d\mathbf{k} \tag{3.6}$$

$$t_j(\mathbf{R}) = \int T_j(\mathbf{k})\,\exp(i\mathbf{k}\cdot\mathbf{R})\,d\mathbf{k} \tag{3.7}$$

Then

$$(k^2 - i\mathbf{k}\cdot\mathbf{L}_j{}^0 + i\omega\gamma_j)H_j = -T_j - z_jH \tag{3.8}$$

where

$$H(\mathbf{k}) \equiv \sum_{i=1}^{I} Z_iH_i(\mathbf{k}) \tag{3.9}$$

Equation 3.8 is an algebraic equation for the $H_j(\mathbf{k})$. It may be solved first for H_j in terms of H and the T_j. Then the solution for H_j may be summed and H computed. Elimination of H then gives H_j in terms of all T_i. The result may be put in the form

$$H_j = -\frac{[T_jO_j + \sum_i (z_iT_j - z_jT_i)Z_iO_{ij}]}{O + \sum_i z_iZ_iO_i} \tag{3.10}$$

where the quantities O, O_i, and O_{ij} are defined in terms of o_i,

$$o_i \equiv i\omega\gamma_i - i\mathbf{k}\cdot\mathbf{L}_i{}^0 \tag{3.11}$$

as follows

$$\begin{aligned} O &\equiv \prod_{i=1}^{I}(k^2 + o_i) \\ O_i &\equiv O[k^2 + o_i]^{-1} \\ O_{ij} &\equiv O_i[k^2 + o_j]^{-1} \end{aligned} \tag{3.12}$$

We make several observations about eq 3.10. First, the right-hand side contains a sum over i that does not con-

tribute at all to the charge transform H. When eq 3.10 is multiplied by Z_j and summed, to get H, the sum over i in (3.10) is annihilated. Second, the inverse transform of H_j will be computed later by residue integration techniques, and all poles of H_j will be assumed to belong to the denominator of (3.10), rather than to the source functions T_i. Lastly, as all the $\mathbf{L}_j^0$ are assumed to lie along the z axis, it is natural to adopt cylindrical coordinates, say $(\mathbf{k}_r,k_z)$. The solution is independent of the cylinder angle coordinate. Then the denominator of (3.10) is a low-order polynomial in k_r^2 (a quadratic polynomial if $I = 2$), and the inverse transform may be reduced to a one-dimensional integral.

These observations can be used immediately to provide some justification of a multipole expansion of the electrostatic potential. It is apparent that such an expansion has to be regarded with considerable suspicion, because the concentration potentials h_i show power law decay in the limit of small applied fields. We suppose that what is required for the validity of a multipole expansion is the existence of all moments M_n of the asymptotic charge.

$$M_n \equiv \int Z^n h(\mathbf{R})\, d\mathbf{R} \tag{3.13}$$

The M_n may be computed from the Fourier transform $H(\mathbf{k})$ as

$$M_n = \int\int Z^n H(\mathbf{k}) \exp(i\mathbf{k}\cdot\mathbf{R})\, d\mathbf{k}\, d\mathbf{R} \tag{3.14}$$

and eq 3.10 gives

$$M_n = -\int\int Z^n \Big(\sum_j Z_j T_j O_j\Big)\Big(O + \sum_j z_j Z_j O_j\Big)^{-1} \exp(i\mathbf{k}\cdot\mathbf{R})\, d\mathbf{k}\, d\mathbf{R} \tag{3.15}$$

Introduction of the cylindrical coordinates $(\mathbf{k}_r,k_z)$ for $\mathbf{k}$ and $(\mathbf{r},z)$ for $\mathbf{R}$ allows a preliminary two-dimensional integration over $\mathbf{r}$. This develops a δ function $\delta(\mathbf{k}_r)$. Thus

$$M_n = -4\pi^2 \int\int Z^n \times \frac{\sum_j Z_j T_j(k_z)(k_z^2 + i\omega\gamma_j - ik_z L_j^0)^{-1}}{1 + \sum_j z_j Z_j (k_z^2 + i\omega\gamma_j - ik_z L_j^0)^{-1}} \exp(ik_z Z)\, dk_z\, dZ \tag{3.16}$$

Integration over z develops the nth derivative of a δ function $\delta(k_z)$.

$$M_n = -8\pi^3 i^n \left[\frac{\partial^n}{\partial k_z^n} \frac{\sum_j Z_j T_j(k_z)(k_z^2 + i\omega\gamma_j - ik_z L_j^0)^{-1}}{1 + \sum_j z_j Z_j (k_z^2 + i\omega\gamma_j - ik_z L_j^0)^{-1}} \right]_{k_z=0} \tag{3.17}$$

In discussing the existence of the derivatives, we first recall the two cases of interest: (1) linear oscillatory flow, for which the $L_j^0 = 0$, and (2) nonlinear steady-state flow, for which $\omega = 0$. Next recall that $t_j(\mathbf{R})$ is intended to be a short-range source. It follows that its Fourier transform evaluated at $\mathbf{k}_r = 0$, namely, $T_j(k_z)$, is a well-behaved funtion of k_z near $k_z = 0$. Later, in section V, a power series expansion will be used. The remaining factor in eq 3.17 also has finite derivatives of all order at $k_z = 0$, and all moments are finite. The only possible divergence of the moments occurs for $n > 1$ in the limit of vanishing frequency (case 1) or vanishing applied field (case 2). As the higher moments have no special interest, especially in those limiting cases where the numerical work presents no difficulty, further discussion has not seemed necessary.

B. Surface Boundary Conditions. On the macroion surface let $R = \kappa a = \alpha$. The electrostatic potential and the normal component of the electric displacement vector are continuous at the surface, so

$$\phi(\alpha^+) = \phi(\alpha^-) \tag{3.18}$$

and

$$(\partial\phi(R)/\partial R)_{\alpha^+} = (D_I/D)(\partial\phi(R)/\partial R)_{\alpha^-} \tag{3.19}$$

where D_I is the dielectric constant inside the sphere. The equilibrium potential is characterized by its reduced ζ potential $\psi^e(\alpha) = \zeta_R$.

The normal components of the velocity and diffusion fluxes are required to vanish on the surface. Therefore

$$(\partial p_i/\partial R)_\alpha = 0 \tag{3.20}$$

and

$$(\partial s/\partial c)_\alpha = 0 \quad \text{or} \quad s(\alpha) = 0 \tag{3.21}$$

according to eq 2.52 and 2.53. The former equation only establishes that s is a constant on the surface. The latter equation establishes that an angle-independent integration constant of s has to be independent of R; otherwise u_θ blows up at $\theta = 0$ and π. So the constant may be chosen as zero.

It is conventional in electrophoretic theory to take the tangential component of velocity to vanish on the surface. However, use of the stream function makes it fairly easy to consider a more general boundary condition involving partial slip. The degree of slipping is determined by a new physical parameter, the "coefficient of sliding friction" f. So as not to lose track of the dimensions or probable order of magnitude of f, we begin consideration of it in physical rather than dimensionless units. Take[12]

$$f v_\theta = \sigma_{r\theta}^{H} + \chi\sigma_{r\theta}^{E}; \qquad R = \alpha \tag{3.22}$$

χ is another parameter which has been set to zero in the numerical work. We next discuss why this was done.

The reason for ascribing slippage at the surface solely to the velocity gradient is that the electrical stress, if retained in eq 3.22 with χ nonvanishing, sets the fluid in motion in circumstances that violate intuition. Consider an uncharged sphere in a nonelectrolyte solution subjected to a constant external electrical field. The divergence of σ^E vanishes, and therefore there is no electrical force appearing in the Navier–Stokes equation. Yet

$$\sigma_{r\theta}^{E} = (D/4\pi)E_r E_\theta \tag{3.23}$$

is nonvanishing. The integral of the normal stress over the surface of the sphere vanishes, in accord with intuition, but locally $\sigma_{r\theta}^E$ is not always zero. Consequently, retention of nonvanishing χ would, in this situation, give rise to motion of the fluid. Such a result does not seem acceptable. We have therefore retained only formally the electrical contribution in eq 3.22 and put $\chi = 0$ in practice. It may well be that nonvanishing values should be considered for electrolyte systems, but we have no estimates to supply, and it has seemed fruitless to explore a set of random numbers.

Little help is available for f either, but some investigation of fluid boundary conditions has taken place.[11] All that we have done is to compare the relative effects of f in the electrolyte problem and in Stokes law for nonelectrolyte systems. The dimensions of f are evidently the same as the dimensions of η/l_f, where l_f is some length, and we take $f = \eta/l_f$. For a nonelectrolyte solvent the effective Stokes law radius a_{eff} becomes[12]

$$a_{eff} = a(1 + 2l_f/a)/(1 + 3l_f/a) \sim a - l_f + \ldots \tag{3.24}$$

and slippage becomes unimportant if $l_f \ll a$. We assume that l_f has the order of magnitude of angstroms.

Application of eq 3.22 requires the following component of σ^H on the surface:

$$\sigma_{r\theta}{}^H = \eta\left[\frac{1}{r}\frac{\partial v_r}{\partial \theta} + r\frac{\partial}{\partial r}\left(\frac{v_\theta}{r}\right)\right] \tag{3.25}$$

The first term in brackets in (3.25) vanishes on the surface. Conversion to dimensionless variables and introduction of the streaming function and electric potential lead to the following form for eq 3.22:

$$\left(\frac{\partial s}{\partial R}\right)_\alpha = \alpha(l_f/a)\left[R^2\frac{\partial}{\partial R}\left(R^{-2}\frac{\partial s}{\partial R}\right) - \frac{3}{2}\chi \sin^2\theta\frac{\partial \psi}{\partial R}\frac{\partial \phi}{\partial c}\right]_\alpha \tag{3.26}$$

IV. Multipole Expansions of Equations

We have found that the charge density decays sufficiently rapidly that its moments exist and concluded that multipole expansions of ϕ and s would therefore be possible. In this section the appropriate expansions are derived. The different fields are all coupled in the problems of interest, so there is no obvious order of presentation.

In order to avoid future repetition of the basic equations, we will treat the linear oscillatory problem and the nonlinear steady-state problem together in this section. A time dependence $\exp(i\omega\tau)$ is assumed for all fields, and $\exp(i\omega\tau)$ is factored out as if the equations were linear. Obviously this is permissible only if any nonlinear terms in $\exp(i\omega\tau)$ are discarded, or if $\omega = 0$, and the equations are valid only in those two special limits. The equations of this section are believed to remain valid in the situation that a weak oscillatory field is superposed on a strong steady field in the same direction, if linearization with respect to the weak field is performed. However, the resultant equations have not been explored.

The multipole expansions are

$$h_i(R,c) \cong \sum_0^L h_i{}^n(R)P_n(c) \tag{4.1}$$

$$\phi(R,c) \cong \sum_0^L \phi^n(R)P_n(c) \tag{4.2}$$

$$s(R,c) \cong \sum_2^G s^n(R)G_n(c) \tag{4.3}$$

where $P_n(c)$ is the Legendre polynomial in $c = \cos\theta$ and $G_n(c)$ is a Gegenbauer polynomial. These polynomials are eigenfunctions of $\nabla_R{}^2$ and $\mathcal{N}$, the latter defined in eq 2.55. Specifically,

$$\nabla_R{}^2[\phi^n(R)P_n(c)] = P_n(c)\mathcal{L}_n\phi^n(R) \tag{4.4}$$

where the operator $\mathcal{L}_n$ is defined by

$$\mathcal{L}_n \equiv \frac{1}{R^2}\left[\frac{\partial}{\partial R}R^2\frac{\partial}{\partial R} - n(n+1)\right] \tag{4.5}$$

and

$$\mathcal{N}[s^n(R)G_n(c)] = G_n(c)\mathcal{N}_n s^n(R) \tag{4.6}$$

where the operator $\mathcal{N}_n$ is defined by

$$\mathcal{N}_n = \frac{\partial^2}{\partial R^2} - \frac{n(n+1)}{R^2} \tag{4.7}$$

The expansion of $p_i{}^n(R,c)$ has the same form as eq 4.1, but $p_i{}^n$ will be obtained from $p_i{}^n = h_i{}^n + z_i\phi^n$. Separate consideration of $p_i{}^n$ is not required.

The upper limits to the sums in (4.1) to (4.3) are dictated by the requirements of numerical precision for the nonlinear problem. For the linear problem only $n = 1$ occurs in (4.1) and (4.2) and $n = 2$ in (4.3). The exclusion of $n = 0$ and $n = 1$ in eq 4.3 results from the boundary condition that the tangential velocity is finite. The $s_n(R)$ cannot depend on R, for $n = 0$ and $n = 1$, according to eq 2.53, and we are therefore free to set their constant values to zero. The G_n for $n > 1$ form a complete and orthonormal basis for functions satisfying the boundary condition of finite velocity. The properties of G_n are summarized in Happel and Brenner[12] and are briefly recapitulated in Appendix A.

Application of the orthonormality and completeness properties of the two basis sets is facilitated with the following definitions of projection operators. $\mathcal{P}_n$ is defined to give δ_{nm} when applied to the Legendre polynomial $P_m(c)$, and $\mathcal{G}_n$ is defined to give δ_{nm} when applied to $G_m(c)/\sin^2\theta$ with n and m greater than unity.

$$\mathcal{P}_n f(c) \equiv \tfrac{1}{2}(2n+1)\int_{-1}^{1} P_n(c)f(c)\,dc \tag{4.8}$$

$$\mathcal{G}_n f(c) \equiv \tfrac{1}{2}n(n-1)(2n-1)\int_{-1}^{1} G_n(c)f(c)\,dc \tag{4.9}$$

When the projections of nonlinear products or exponentials of fields were required in the numerical work, eq 4.8 and 4.9 were replaced by Gauss–Legendre numerical integrations.

For clarity regarding the two limiting situations defined at the beginning of this section, as well as for numerical accuracy, it is useful to have a distinct separation between linear and nonlinear contributions. This is the reason for breaking up the source terms in the following equations in what might seem a needlessly complicated way.

Our plan is to present the differential equations for the various fields initially and then return to the Legendre or Gegenbauer decomposition of the boundary conditions. In each case the differential equations will be written with $\mathcal{L}_n$ or $\mathcal{N}_n$ acting on one of the fields on the left side and a defined source term on the right.

A. Electrical Potential. Equations 2.43 and 2.45 give, after the equilibrium potential and charge density are subtracted,

$$\nabla_R{}^2\phi = -\sum_i Z_i \exp(-z_i\psi^e)(-1 + \exp h_i) \tag{4.10}$$

Application of $\mathcal{P}_n$ to this equation gives

$$\mathcal{L}_n\phi^n = F^n(R) \tag{4.11}$$

where

$$F^n(R) \equiv -\sum_i Z_i h_i{}^n \exp(-z_i\psi^e) - \sum_i Z_i \exp(-z_i\psi^e)\mathcal{P}_n(-1 - h_i + \exp h_i) \tag{4.12}$$

The source term F_n is here divided into a linear part, the first sum on the right-hand side, and a nonlinear part which is at least quadratic in applied fields.

B. Electrochemical Potentials. In eq 2.49 the time dependence is taken to be $\exp(i\omega\tau)$. We recall our understanding that linearization with respect to the oscillatory part of the field is implicit. In the term $\nabla_R{}^2 p_i$ of eq 2.49, p_i is replaced by $h_i + z_i\phi$, and eq 4.10 and 4.11 are used. Projection with $\mathcal{P}_n$ gives

$$\mathcal{L}_n h_i{}^n = H_i{}^n(R) \tag{4.13}$$

where

$$H_n{}^i(R) = i\omega\gamma_i h_i{}^n + z_i\frac{\partial \psi^e}{\partial R}\left[\gamma_i\frac{s^{n+1}}{R^2} + \frac{\partial p_i{}^n}{\partial R}\right] - z_i F^n + \mathcal{P}_n[\nabla_R h_i \cdot(\gamma_i \mathbf{u} - \nabla_R p_i)] \tag{4.14}$$

The projection of the radial velocity component has been written as

$$\mathcal{P}_n u_R = -R^{-2} s^{n+1}(R) \tag{4.15}$$

which readily follows from the fact that $dG_n/dc = -P_{n-1}$. The nonlinear parts of the source H_i^n are the nonlinear part of F^n and the last term on the right side of (4.14). That term retains an explicit projection operator. Written out in terms of the potentials and their derivatives, the last term takes the form

$$\mathcal{P}_n[\nabla_R h_i \cdot (\gamma_i \mathbf{u} - \nabla_R p_i)] = \frac{1}{R^2}\mathcal{P}_n\left[\left(\gamma_i \frac{\partial s}{\partial c} - R^2 \frac{\partial p_i}{\partial R}\right)\frac{\partial h_i}{\partial R} - \left(\gamma_i \frac{\partial s}{\partial R} + \sin^2\theta \frac{\partial p_i}{\partial c}\right)\frac{\partial h_i}{\partial c}\right] \tag{4.16}$$

C. Stream Function. Application of the projection operator $\mathcal{G}_n$ to eq 2.57 after division by $\sin^2\theta$ gives

$$\mathcal{N}_n^2 s^n = S^n(R) \tag{4.17}$$

where

$$S^n(R) \equiv \tfrac{3}{2}\sum_i Z_i \exp(-z_i\psi^e)\mathcal{G}_n\left[(\exp h_i)\left(\frac{\partial p_i}{\partial c}\frac{\partial \psi}{\partial R} - \frac{\partial p_i}{\partial R}\frac{\partial \psi}{\partial c}\right)\right] \tag{4.18}$$

It will be convenient for some purposes to write the fourth-order differential equation for the stream function, eq 4.17, as a pair of second-order differential equations for s^n and the auxiliary function w^n defined by

$$\mathcal{N}_n s^n = w^n(R) \tag{4.19}$$

and

$$\mathcal{N}_n w^n = S^n(R) \tag{4.20}$$

Finally, it is convenient to have the source term S^n explicitly divided into its linear and nonlinear parts. Equation 4.18 gives

$$S^n(R) = \tfrac{3}{2}n(n-1)\sum_i Z_i \exp(-z_i\psi^e)(\partial\psi^e/\partial R)p_i^{n-1} + \tfrac{3}{2}\sum_i Z_i \exp(-z_i\psi^e)\left\{\frac{\partial\psi^e}{\partial R}\mathcal{G}_n(-1 + \exp h_i)\frac{\partial p_i}{\partial c} + \mathcal{G}_n\left[(\exp h_i)\left(\frac{\partial h_i}{\partial c}\frac{\partial \phi}{\partial R} - \frac{\partial h_i}{\partial R}\frac{\partial \phi}{\partial c}\right)\right]\right\} \tag{4.21}$$

The first sum on the right-hand side is linear, and the remaining terms are quadratic or higher order in the applied fields.

V. Multipole Expansion of Boundary Conditions

We take up first the behavior of the solutions at large R and then the boundary conditions on the macroion surface. A preliminary discussion of asymptotic behavior was presented in section III. That discussion has now to be amplified in the context of the truncated multipole expansions developed in section IV.

The asymptotic concentration potentials h_j^n satisfy a set of differential equations (3.5) that do not involve the electrostatic potential or any aspect of the stream function other than the electrophoretic velocity $\mathbf{U}^0$. The order of discussion, therefore, is the concentration potentials first, followed by a special discussion of charge decay, then the electrostatic potential, and last the stream function.

A. Asymptotic Expansions of Concentration Potentials. The concentration potential $h_j(\mathbf{R})$, $1 \le j \le I$, is given in eq 3.6 as the Fourier transform of $H_j(\mathbf{k})$, and the latter is given in eq 3.10. It proves convenient later to deal with a displaced wave vector $\mathbf{w}$. Let

$$\mathbf{w} \equiv \mathbf{k} + i\mathbf{M}$$
$$\mathbf{F}_j(\mathbf{w}) \equiv \mathbf{H}_j(w - i\mathbf{M}) \tag{5.1}$$
$$h_j(\mathbf{R}) \equiv \exp(\mathbf{M}\cdot\mathbf{R}) f_j(\mathbf{R})$$

where

$$f_j(\mathbf{R}) = \int F_j(\mathbf{w}) \exp(i\mathbf{w}\cdot\mathbf{R})\, d\mathbf{w} \tag{5.2}$$

The displacement $\mathbf{M}$ is a constant vector that will be chosen later to facilitate a residue integration of eq 5.2.

All functions will retain the axial symmetry of the physical problem, and in spherical polar coordinates $\mathbf{w} = (w,\theta_w,\varphi_w)$, F_j will be independent of the azimuthal angle. The spherical harmonic addition theorem may therefore be used in the form[14]

$$\int_0^{2\pi} \exp(i\mathbf{w}\cdot\mathbf{R})\, d\varphi_w = 2\pi\sum_0^\infty (2n+1) i^n P_n(\cos\theta_R) P_n(\cos\theta_w) j_n(wR) \tag{5.3}$$

where $j_n(wR)$ is a spherical Bessel function of the first kind.[14,15] It follows from eq 5.2 that

$$f_j(\mathbf{R}) = \sum_0^\infty f_j^n(R) P_n(\cos\theta_R) \tag{5.4}$$

where

$$f_j^n(R) = 4\pi i^n \int_0^\infty j_n(wR)\mathcal{P}_n F_j(\mathbf{w}) w^2\, dw \tag{5.5}$$

The projection operator $\mathcal{P}_n$ here operates on θ_w.

The integrand in eq 5.5 is an even function of w, and the domain of integration may be extended to the range $-\infty < w < +\infty$. This may be verified from the Fourier inverse of eq 5.2, along with eq 5.3 and

$$j_n(-x) = (-1)^n j_n(x)$$
$$P_n(-c) = (-1)^n P_n(c)$$

Introduction of the spherical Bessel functions of the third kind,[15] $h_n^{(1)}$ and $h_n^{(2)}$,

$$j_n(wR) = \tfrac{1}{2}[h_n^{(1)}(wR) + h_n^{(2)}(wR)] \tag{5.6}$$

gives

$$f_j^n(R) = 2\pi i^n \int_{-\infty}^{+\infty} h_n^{(1)}(wR)\mathcal{P}_n F_j(\mathbf{w}) w^2\, dw \tag{5.7}$$

The last integral will be evaluated by residue integration. It may be verified that the integrand has no poles at the origin except in the linear steady state. The argument is essentially that employed earlier, in section III, to show that the multipole moments of $h_j(\mathbf{R})$ are finite.

We now refer again to eq 3.10 for $H_j(\mathbf{k})$ and write that equation in the form

$$H_j(\mathbf{k}) = \mathcal{N}_j(\mathbf{k})/\mathcal{D}(\mathbf{k}) \tag{5.8}$$

The numerator is defined by

$$\mathcal{N}_j(\mathbf{k}) \equiv -[T_j O_j + \sum_i (z_i T_j - z_j T_i) Z_i O_{ij}] \tag{5.9}$$

and the denominator by

$$\mathcal{D}(\mathbf{k}) \equiv O + \sum_i z_i Z_i O_i \tag{5.10}$$

For the special case $I = 2$, i.e., when two mobile ions are present, the denominator takes the form

$$\mathcal{D}(\mathbf{k}) = k^4 + k^2(1 + o_1 + o_2) + 2i\mathbf{k}\cdot M + i\omega(z_1Z_1\gamma_2 + z_2Z_2y_1) + o_1o_2 \quad (5.11)$$

where

$$\mathbf{M} = -\tfrac{1}{2}(z_1Z_1\mathbf{L}_2^0 + z_2Z_2\mathbf{L}_1^0) \quad (5.12)$$

and the o_i were defined in section III. Equation 5.12 gives the value of the previously arbitrary vector $\mathbf{M}$. The rationale for this choice will appear shortly.

We now make the tentative assumption that all poles in the integrand of eq 5.7 arise from the denominator $\mathcal{D}$ of (5.8), rather than from the source functions T_i in the numerator. The T_i will be considered shortly.

In the special case of linear flow the $\mathbf{L}_j^0$ and $\mathbf{M}$ vanish. For $\omega = 0$ the roots of $\mathcal{D}$ and the poles of F_j occur at $k = 0,i$. For linear oscillatory flow at nonvanishing frequency, $\mathcal{D}$ is still a quadratic function in k^2, so the roots remain easy to calculate. A few details of the resulting formulas are summarized in Appendix B. In view of the recent work by DeLacey and White[6] on linear oscillatory flow, it has seemed appropriate to present only a sketch of that case according to the present approach.

The nonlinear steady-state case, $\omega = 0$, is now considered. For moderate field strengths one of the poles should stay near the origin, and this pole is the one most relevant to the asymptotic behavior. For small k eq 5.11 may be approximated by

$$\mathcal{D}(\mathbf{k}) \cong |\mathbf{k} + i\mathbf{M}|^2 + M^2 = w^2 + M^2 \quad (5.13)$$

and the appropriate root is $w = i\lambda$, where $\lambda = |\mathbf{M}|$. In practice the magnitude of λ is about 0.1–0.2 for the largest field strengths we have considered, namely, $\mathcal{E} \simeq 1$. For such field strengths the numerator $\mathcal{N}_j$ of eq 5.8 can be approximated by

$$\mathcal{N}_j(\mathbf{k}) \cong -\sum_i (z_iT_j - z_jT_i)Z_i \quad (5.14)$$

because O_j is smaller than O_{ij}, which is just unity for $I = 2$, by a factor of order λ^2. It should be appreciated that this approximation completely suppresses the long-range charge density, which is obtained from multiplication of h_j or f_j by Z_j and summation over j. The nature of the long-range charge decay will be considered in more detail below, and a nonvanishing approximation will be given. With eq 5.13 and 5.14, the residue integration for f_j^n may be completed with the result

$$f_j^n = 2\pi^2\lambda i^n h_n^{(1)}(i\lambda R)\mathcal{P}_n\sum_i (z_iT_j - z_jT_i)Z_i \quad (5.15)$$

where the T_j are to be evaluated with $w = i\lambda$.

The T_j have now to be considered. We require $T_j(\mathbf{w} - i\mathbf{M})$ and evaluate it from its Fourier transform relation to the physical sources t_j:

$$T_j(\mathbf{w} - i\mathbf{M}) = (8\pi^3)^{-1}\int \exp(-\mathbf{M}\cdot\mathbf{R} - i\mathbf{w}\cdot\mathbf{R})t_j(\mathbf{R})\, d\mathbf{R} \quad (5.16)$$

A spherical harmonic expansion of $\exp(-i\mathbf{w}\cdot\mathbf{R})$, as in eq 5.3, shows that the integral over $\mathbf{R}$ required in (5.16) is proportional to

$$\int \exp(-\mathbf{M}\cdot\mathbf{R})j_n(wR)P_n(\cos\theta_R)t_j(\mathbf{R})\, d\mathbf{R} \quad (5.17)$$

As our intention has been to generate the asymptotic solutions from short-ranged sources $t_j(\mathbf{R})$, it follows that the j_n may be expanded in powers of wR. The result is

$$\mathcal{P}_nT_j(\mathbf{w} - i\mathbf{M}) \propto (-iw)^n$$

or

$$\mathcal{P}_nT_j(\mathbf{w} - i\mathbf{M}) \propto \lambda^n \quad (5.18)$$

at the pole.

For convenience in the numerical work we have absorbed the proportionality constants in eq 5.18, and other constants in (5.15), into parameters T_j^n and defined the modified Bessel functions of the third king $g_n(\lambda R)$:

$$g_n(\lambda R) \equiv i^{n+2}\lambda^{n+1}h_n^{(1)}(i\lambda R) \quad (5.19)$$

A few relevant properties of the g_n are summarized in Appendix C. Note that in the limit $\lambda \to 0$, $g_n \propto R^{-(n+1)}$.

The final result for f_j^n is

$$f_j^n(R) = g_n(\lambda R)\sum_{i=1}^{I}(z_iT_j^n - z_jT_i^n)Z_j \quad (5.20)$$

Calculation of h_j^n follows eq 5.1,

$$h_j^n(R) = \mathcal{P}_n \exp(\mathbf{M}\cdot\mathbf{R})\sum_{m=0}^{L} f_j^m(R)P_m(\cos\theta R) \quad (5.21)$$

The sum over m is truncated at L because our method of solving the differential equations allows $I\cdot(L + 1)$ parameters for the asymptotic forms of the h_j^n. In fact, eq 5.20 shows that only $(I - 1)\cdot(L + 1)$ independent parameters are present in the approximation being used, because

$$h^n \equiv \sum_j Z_jh_j^n$$

vanishes identically. However, an additional set of $(L + 1)$ parameters will be introduced in the asymptotic description of the h^n.

B. Asymptotic Expansion of the Charge Density. As was noted below eq 5.14, the approximation being used for the concentration fields h_j^n is inadequate for the linear combination of concentrations that gives the charge density. Retention of the discarded terms would not add a great deal of work to the calculation of h_j^n, but that work was not felt to be worthwhile for several reasons, which we now discuss.

First, the charge density is not itself one of the fields to be integrated. Rather the h_j^n fields are the ones to be initiated at the outer boundary, and the missing contributions should be smaller, as was noted, by a factor of about λ^2. The numerical work bore this out: the charge contribution h^n was smaller than individual h_j^n by a factor of 10^2–10^3 at the largest fields and R that were studied. So the improvement in the concentration fields would be small.

Second, a parameterized expression for the charge density at large R is useful mainly for the calculation of the multipole moments of charge and dipole moment. Because the charge density decays with R quite slowly at large field strengths, the asymptotic expansion of the electrical potential is achieved very slowly. Unfortunately, the terms left out of eq 5.14 give rise to an $h^n(R)$ that seems impossible to integrate analytically, and painful to integrate numerically.

Third, and most important, it seemed quite doubtful that the asymptotic expression for h^n would give an adequate account of the charge density even it it were easy to integrate it. The numerical integration results indicated that the linear contribution to the charge density, namely, h^n, accounted for only $^1/_2$ to $^2/_3$ of the total charge density at the largest R practical to study by the methods of section VI. The maximum feasible distance from the inner to the outer boundary was about 12–18 Debye lengths with those methods.

For these reasons $h^n(R)$ was arbitrarily assigned a power law decay, and the coefficients of the $(L + 1)$ power functions provided the remaining parameters at the outer

boundary. h^n was treated as if it were the proper charge density at large R for the purpose of extrapolating the multipole moments. And finally, the adequacy of the choice of powers was judged by whether the extrapolated estimates of the charge and dipole moments approached constant values in the outer range of numerical integration. The approximation is not very good as small fields, but the outer boundary could be taken far enough out that good agreement with the linearized theory of Appendix B was obtained. At large fields the approximation seemed to work better. The concluding discussion of results will put these last remarks in more quantitative terms.

The specific equations used were

$$\mathcal{L}_n\phi_h{}^n \sim -h^n$$

$$h^n \sim R^{-(3+n+x)}; \qquad \phi_h{}^n \sim R^{-(1+n+x)} \tag{5.22}$$

and x varied with n. According to the discussion in section III, all the moments of charge distribution should exist for nonvanishing fields. It suffices to take $x > 0$ for this purpose. In practice we generally used $x = (1, 1, 0.1, 0.1)$ for $n = (0, 1, 2, 3)$, respectively.

C. Remaining Asymptotic Expansions. The source terms F^n and S^n on the right-hand sides of the basic differential equations (4.11) and (4.20) will have exponential decay at infinity for finite field strengths. The solutions of those equations will therefore behave at infinity like the solutions of the corresponding homogeneous equations. These equations involve the operators $\mathcal{L}_n$ and $\mathcal{N}_n$.

The operator $\mathcal{L}_n$ has the power law eigenfunctions

$$\mathcal{L}_nR^m = 0; \qquad m = n, -(n+1) \tag{5.23}$$

and $\mathcal{N}_n$ has the eigenfunctions

$$\mathcal{N}_nR^m = 0, \qquad m = n, \qquad 1-n \tag{5.24}$$

As just noted, we add $\phi_h{}^n$ of (5.22) to the multiple solution for ϕ^n:

$$\phi^n(R) \sim -\mathcal{E}^0R\delta_{n,1} + A^nR^{-(n+1)} + \phi_h{}^n(R) \tag{5.25}$$

The first term on the right-hand side gives the applied field, and the second term gives the multipole field. The latter for $n = 0$, $n = 1$ are related to the apparent charge and dipole moment introduced earlier in eq 2.12:

$$A^0 = eq\kappa/k_BTD = q_R \tag{5.26}$$

$$A^1 = \mu e\kappa^2/k_BTD = \mu_R \tag{5.27}$$

with $\mu = \mu\mathbf{e}_z$. q_R and μ_R are the apparent induced charge and dipole moment, in reduced units. They will be tabulated for a few examples below.

The equation for the velocity potential s^n has been split into eq 4.19 and 4.20. The latter has the source term S^n and has the asymptotic solutions of the homogeneous equation, R^n and R^{1-n}. The first of these generates a solution of (4.19), $s^n \sim R^{n+2}$. This has to be rejected because it leads to a divergent velocity, and

$$w^n \sim 2(3-2n)W^nR^{1-n} \tag{5.28}$$

A multiplicative constant has been inserted here so that it does not appear later. Substitution from eq 5.28 into eq 4.19 generates a special solution of the latter, and addition of the two general solutions gives

$$s^n \sim S_1{}^nR^n + S_2{}^nR^{1-n} + W^nR^{3-n} \tag{5.29}$$

The requirement that the velocity approaches a constant at infinity gives

$$S_1{}^n \equiv 0, \qquad n > 2 \tag{5.30}$$

Equation 5.29 adds two parameters at the outer boundary for each $n > 2$. Two boundary conditions at $R = \kappa a$ will later be added also for each $n > 2$.

For $n = 2$ the parameter W^n is not free; it is determined in terms of the centrifugal force and the charge q from eq 2.16. To establish this connection and the physical interpretation of $S_1{}^2$, we express eq 2.8 and 2.16 in dimensionless variables:

$$\mathbf{u} \sim -\mathbf{U}^0 - (3\mathcal{B}F^H/4k_BT)R^{-1}(1 + \mathbf{e}_R\mathbf{e}_R)\cdot\mathbf{e}_z \tag{5.31}$$

Comparison of this expression with the expression for u derived from eq 2.52, 2.53, and 5.29 gives

$$S_1{}^2 = U^0 \tag{5.32}$$

and

$$W^2 = -\tfrac{3}{2}(\mathcal{B}/k_BT)(qE^0 + F^g) \tag{5.33}$$

or

$$W^2 = -\tfrac{3}{2}[A^0\mathcal{E}^0 + \mathcal{B}F^g/k_BT] \tag{5.34}$$

with the aid of eq 5.26 for A^0 and eq 2.38 for $\mathcal{E}^0$. $\mathcal{E}^0$ and F^g designate projections on the positive z axis. For $n = 2$, then, the parameters to be added to the list of unknowns are $S_1{}^2$ and $S_2{}^2$, and the first of these is equal to the electrophoretic velocity. (It has been conventional in theoretical studies of the linear electrophoretic velocity to express the results as the dimensionless reduced mobility $U^0/\mathcal{E}^0$.)

D. Inner Boundary Conditions. For every parameter introduced at the outer boundary, an equation without additional unknowns has to be specified at the inner boundary. Since all fields in the vicinity of the inner boundary are in principle known in terms of the previous parameters, from solutions to the differential equations, the fields themselves do not contain additional unknowns.

For the electrostatic potential, eq 3.17 and 3.18 provide two equations and two additional parameters, the inner field and its derivative. However, the latter are related

$$\phi^n(R) \propto R^n, \qquad R < \alpha \tag{5.35}$$

and this yields the single equation with no new parameters

$$(\partial\phi^n(R)/\partial R)_\alpha = n(D_1/D)\alpha^{-1}\phi^n(\alpha) \tag{5.36}$$

The derivative at $R = \alpha$ has to be evaluated on the solution side of the macroion surface.

The condition of vanishing diffusion flux gives

$$(\partial p_i{}^n/\partial R)_\alpha = (\partial h_i{}^n/\partial R)_\alpha + z_i(\partial\phi^n/\partial R)_\alpha = 0 \tag{5.37}$$

The condition of vanishing normal solution velocity gives, from eq 3.20,

$$s^n(\alpha) = 0 \tag{5.38}$$

There remains the boundary condition (3.25) involving sliding friction. Division of that equation by $\sin^2\theta$ and application of the projection operator $\mathcal{G}_n$ gives

$$(\partial s^n/\partial R)_\alpha = \alpha(l_f/a)\left[R^2\frac{\partial}{\partial R}\left(R^{-2}\frac{\partial s^n}{\partial R}\right) - \tfrac{3}{2}xn(n-1)\frac{\partial\psi^e}{\partial R}\phi^{n-1} - \tfrac{3}{2}x\mathcal{G}_n\frac{\partial\phi}{\partial R}\frac{\partial\phi}{\partial c}\right]_\alpha \tag{5.39}$$

The last term on the right-hand side is quadratic or higher order in the applied fields. Preceding terms are linear (or higher) order.

VI. Numerical Aspects

A count of the second-order differential equations provides a useful introduction to the discussion of numerical work. We have one ordinary second-order differential

equation for $\psi^e(R)$, one partial differential equation for each concentration field $h_i(R,\theta)$, with $i = 1, ..., I$, two equations for the velocity, involving the stream function $s(R,\theta)$ and the auxiliary function $w(R,\theta)$, and one equation for the electrostatic potential $\phi(R,\theta)$. The expansions of h_i and ϕ in $(L + 1)$ Legendre polynomials and s and w in $(G - 1)$ Gegenbauer polynomials raises the count to $[(I + 1)(L + 1) + 2(G - 1) + 1]$ ordinary second-order equations, or twice as many first-order equations. For most of the numerical work, only two salt species were used, and the multipole expansions were truncated at $L = G = 3$. This seemed adequate at least for preliminary work. These values generate 34 first-order equations. The equations are nonlinear and are of elliptic type, apparently well-known to be numerically unstable. The equations for $\psi^e(R)$ can be solved independently; the remaining equations are coupled to each other and to $\psi^e(R)$. So the numerical problems were nontrivial, by the standards of the author.

The goal of the numerical work is to satisfy the boundary conditions at some large R, say, $R = \beta$, with a set of parameters described in section V. Some of these parameters, such as the velocity $\mathbf{U}^0$ and the dipole moment μ_R, have direct physical interest. All the parameters have to be chosed so that the boundary conditions at the surface $R = \alpha$ are satisfied. In principle the number of parameters is half the number of first-order differential equations.

In the following paragraphs we first discuss the most elementary form of the "shooting method" used to determine the parameters and then sketch a slight refinement of it that increases the stability of the algorithm. Transformations of the differential equations, made for the same purpose, are then summarized.

A. Shooting Method. This method was used before for the linear electrophoresis and conductivity problems[5,6] but was not so named. Lengthy descriptions[16,17] and brief summaries[18] may be found in the literature. In its simplest form the method supposes that parameters $P^b = [P_i^b]$, $i = 1, ..., p$, specify the values of certain functions $y_i(R)$, here $2p$ in number, at $R = \beta$. The y_i satisfy a set of $2p$ first-order differential equations that may be integrated from $R = \beta$ to $R = \alpha$. The y's at $R = \alpha$ are then functions of the P_i^b, and p boundary conditions at α give rise to p equations

$$F_i(P^b,\alpha) = 0, \qquad i = 1, ..., p \tag{6.1}$$

that have to be solved for the P_i^b. If the differential equations are linear in those y's that depend on the P_i^b, then the algebraic equations (6.1) are linear in the P_i^b. Nonlinear differential equations give rise to nonlinear algebraic equations that may be solved, if one is fortunate, by a Newton iteration of eq 6.1. This is the procedure we followed. A finite difference estimate of the Jacobian $[\partial F_i/\partial P_j^b]$ was used for the iteration. To compute the differences in F_i, p integrations of the set of differential equations are needed, a different P_j^b being varied for each integration, and one integration must be performed with unvaried P's. This iteration is not guaranteed to converge in the absence of a good initial approximation. However, in the problem at hand results were needed for a range of external fields, starting from very weak fields, where the equations are nearly linear, and ranging upward. So reasonably good initial approximations to P^b were available by extrapolation of values obtained for weaker fields.

The simple shooting method did not work very well for nonlinear problems, presumably because of the instability of the underlying differential equations. Therefore recourse was had to a modification, also described in the literature, that reduces the range over which the differential equations need be integrated. Instead of solving for just p parameters P^b that determine all y_i at β, a second set of parameters P^a was introduced that was sufficient, when coupled with the known boundary conditions, to determine all the y's at $R = \alpha$. The differential equations are then integrated once from α and once from β to a common "matching point" R_M, where continuity of all y's gives $2p$ equations

$$F_i(P^a,P^b,R_M) = 0, \qquad i = 1, ..., 2p \tag{6.2}$$

This procedure may be considered a simple version of multiple or parallel shooting.[16-18] It may seem perverse to double the number of unknowns, but the improvement in stability of the algorithm was quite considerable. Even under conditions where either set of equations could be used, the second set requires less accurate solutions of the differential equations and therefore may require less computer time.

B. Differential Equations. With increasing order of the Legendre or Gegenbauer expansions, the n dependent parts of the differential operators $\mathcal{L}_n$ and $\mathcal{N}_n$, in eq 4.5 and 4.7, respectively, seemed quite threatening to numerical stability. Consequently all the second-order differential equations were transformed using the method of "variation of constants". In summary, a solution y for one of the unknown functions of R, for example, $s^n(R)$, is written in the form

$$y(R) = Y_1(R)y_1(R) + Y_2(R)y_2(R) \tag{6.3}$$

and

$$Y_1'y_1 + Y_2'y_2 = 0 \tag{6.4}$$

is imposed as a constraint on the Y's. y_1 and y_2 are solutions of the homogeneous equation. For our equations, y_1 and y_2 were powers of R, as discussed in the preceding section. Further details of these transformations are recorded in Appendix D.

VII. Results and Discussion

In this section we examine the numerical results. Only a few samples are shown, sufficient to indicate orders of magnitude and trends. A physical picture that makes all the phenomena qualitatively self-evident has yet to be found, but more or less plausible rationalizations are offered. Lastly, a conversion between reduced and physical units will be performed, to illustrate the actual magnitude of the change in conductivity.

Numerical results for the induced charge and dipole moment are illustrated in Figures 1 and 2 for a "small" sphere, $\kappa a = 3$ and $\zeta_R = 4$, and in Figures 3 and 4 for a "large" sphere, $\kappa a = 50$ and $\zeta_R = 6$. The latter figures also show the striking effects that result from solvent slippage at the macroion surface. We discuss the results in more detail in connection with a physical description of the underlying processes.

A. Physical Analysis. Figure 5 illustrates a positively charged macroion in an external applied field $\mathbf{E}^0$. The + and − signs indicate the various physical charges to be discussed. Encircled + and − signs indicate a net charge density that results from the movement of ions into or out of a particular region of space. The numbers in Figure 5 identify positions to be discussed. The convention is adopted that a primed number (not shown on the figure to avoid clutter) is the mirror image of the unprimed number. Thus, a negatively charged plate at 1 and a positively charged plate at 1′ create an applied field $\mathbf{E}^0$ in the positive (upward) direction (2). The positive macroion at 5 moves upward with the electrophoretic velocity $\mathbf{U}^0$.

We assign effects that show up with increasing field strength to the linear, weakly nonlinear, and strongly

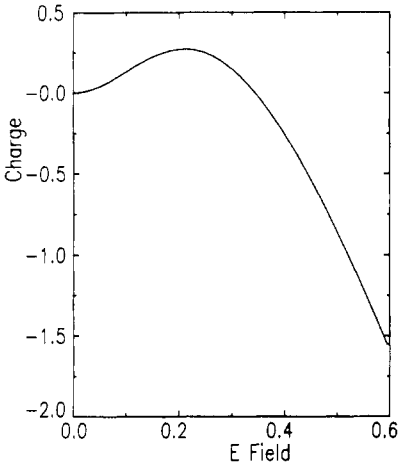

Figure 1. Reduced charge q_R vs. field strength $\mathcal{E}^0$. Parameters were $\kappa a = 3$, $\zeta_R = 4$, $D_I = 0$, and $l_f/a = 0$ (no slip).

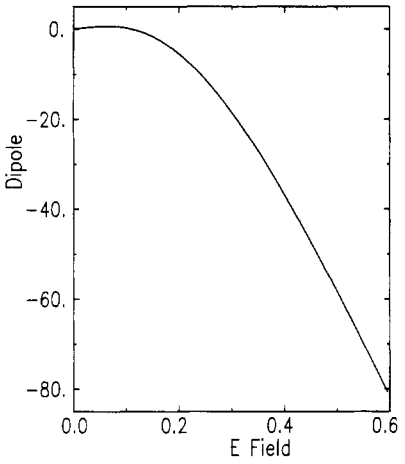

Figure 2. Reduced dipole moment μ_R vs. field strength. Parameters as in Figure 1.

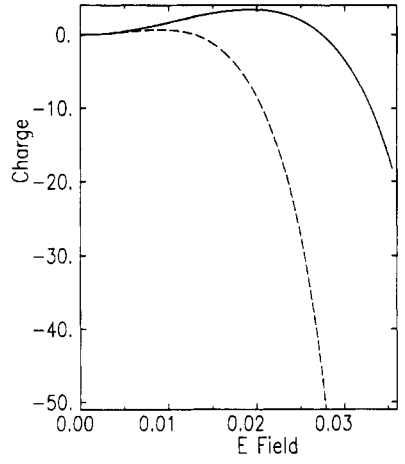

Figure 3. Reduced charge vs. field strength for $\kappa a = 50$, $\zeta_R = 6$, and $D_I = 0$. Solid curve is for no slip, $l_f/a = 0$, and dashed curve is for partial slip, $l_f/a = 0.01$.

nonlinear regimes of applied field strengths.

1. Linear Regime. a. Maxwell–Wagner Effect. Consider first the uncharged sphere, $\zeta_R = 0$, in a pure solvent without counterions. Take $D_I = 0$. Then the boundary condition on the normal component of electrical field, $\partial\phi/\partial b = 0$, generates a strong negative dipole moment or polarizability. Addition of mobile salt ions has no additional effect if $D_I = 0$, because the boundary condition $\partial\phi/\partial b = 0$ is sufficient to repel entry of the ions into the sphere. If $D_I > 0$, a surface charge builds up in the solution

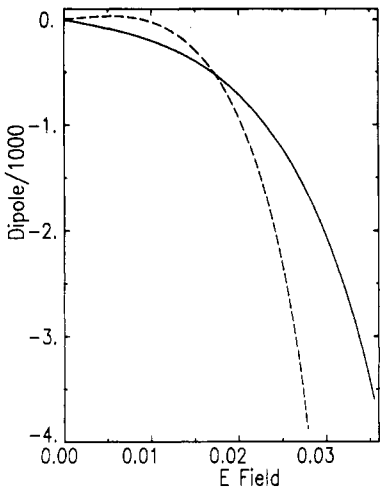

Figure 4. Reduced dipole moment vs. field strength. Parameters as in Figure 3.

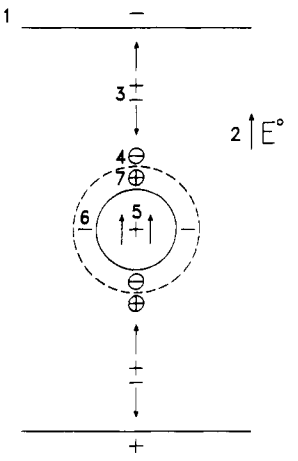

Figure 5. Schematic diagram of mobile ion flows and accumulations.

to maintain the boundary condition $\partial\phi/\partial b$ as a limit on solution values of the normal component. The polarizability of a nonconducting, uncharged sphere in salt solution is the same as that of the sphere in pure water if $D_I = 0$.

b. Ion Atmosphere Polarization. Polarization of the ion atmosphere accumulates counterions, and a negative charge density, at 7′. A deficiency of counterions, or a positive charge density, accumulates at 7. This polarization generates a positive dipole moment.

c. Combination Effects. If κa is small or ζ_R is large, polarization of the double layer dominates, and $\mu_R > 0$. An example is seen in Figure 2 for small field strengths. If κa is large or ζ_R is small, the Maxwell–Wagner effect dominates and $\mu_R < 0$; an example is seen in the solid curve of Figure 4. The dashed curve in Figure 4 shows results for a partial slip boundary condition. The increased convection in the double layer yields additional polarization and makes $\mu_R > 0$.

A second combination effect is the development of a deficiency of (neutral) salt concentration at 3–4, and an excess at 3′–4′. At the bottom of the sphere, counterions flow out and are neutralized by coions flowing upward. Both positive and negative ions accumulate at 3′, in nearly equal amounts at low field strength. Counterions flow out of region 3 into the double layer, and coions flow out of region 3 toward the upper plate, resulting in a deficiency of salt concentration there. This is a linear effect but gives no direct contribution to charge or dipole accumulation. The perturbation in concentration is a dipole field and

therefore decays very slowly with distance.

2. Weakly Nonlinear Regime. Figures 1 and 3 show an initial development of positive charge as the field strength increases. This is similar to the classical Wien effect. Convection and electrical forces acting on the distorted ion atmosphere remove counterions faster from the region of accumulation, 7′, than from the depleted region at 7, until, in the steady state, concentration gradients build up to restore a balance. There is no longer sufficient negative charge in the ion atmosphere to compensate the macroion charge, and the macroion + ion atmosphere system has a net positive charge.

The polarizability decreases algebraically in this regime, presumably because the more easily polarized outer parts of the double layer are stripped away.

3. Strongly Nonlinear Regime. At high field strengths Figures 1–4 show a strong buildup of negative charge and negative polarizability. The algebraic decrease in polarizability continues a trend that started in the weakly nonlinear regime.

At least part of the decrease in polarizability can be explained as in 2. If the more easily polarized parts of the double layer are stripped away, the positive contribution from the ion atmosphere is lost, and the negative contribution to the polarizability from the Maxwell–Wagner effect predominates.

However, the dipole moments become more negative at strong fields than the Maxwell–Wagner polarizability predicts. So we have to seek some real accumulation of negative charge in regions 4 to 7 and positive charge in regions 4′ to 7′, and the former negative charges must predominate.

A more detailed view of the strongly nonlinear regime was obtained from an examination of the actual charge and concentration fields. The system was that used for Figures 3 and 4, with non-slip boundary conditions and a reduced field of 0.035 (about the largest value shown on the figures). For the first few Debye lengths away from the surface, the charge rearrangement shown in Figure 5 at 7 and 7′ and discussed under 2 is maintained. In strong fields the inner double layer retains its positive polarization and positive net charge. The new phenomena have to be ascribed primarily to the domain 4–4′ outside what would ordinarily be described, in equilibrium, as the double layer. The region of disturbance is quite large: at 10 Debye lengths from the surface the salt concentration still deviates from its bulk value by roughly 50% (positively in region 3′ and negatively in region 3). The negative charge accumulation peaks in the vicinity of 3–4 Debye lengths from the surface.

Apparently the inner part of the ion atmosphere can conduct counterions downward sufficiently rapidly that a steady-state depletion occurs at 7, while the outer region 4, with a weaker conductivity, shows a steady-state accumulation.

B. Physical Units. The relative change ΔK in conductivity due to macroions at number density C_P is[4]

$$\Delta K/K_S = 4\pi C_P \mu/DE^0$$

where K_S is the conductivity of pure salt solution and μ is the dipole moment. In our reduced units this equation can be written

$$\Delta K/K_S = (3\mu_R/\alpha^3\mathcal{E}^0)p$$

where p is the volume fraction of spherical macroions.

The system used for Figures 3 and 4 is considered for a numerical example. Suppose the salt concentration is 10^{-3} M. The Debye length is $\kappa^{-1} \cong 100$ Å, and since $\kappa a = 50$, the radius is about 5000 Å. This is in the range available for polystyrene latex spheres. Take $\mathcal{E}^0 = 0.02$, on the border of the strongly nonlinear regime. This corresponds to about 500 V/cm, according to eq 2.38. Figure 4 gives $\mu_R \cong -700$, and therefore

$$\Delta K/K_S \cong -0.8p$$

A very small p is wanted, since the theory deals strictly with dilute solutions. In sum, it would be necessary to measure roughly 1% changes in the conductivity of 10^{-3} M salt solution to moderate accuracy to test the theory. The required field strengths are fairly low, so pulsed bridge techniques seem likely to be feasible. We can say at least that the conditions seem less severe than apply to the classical Wien effects.[1]

It is remarkable, and perhaps not surprising in retrospect, that nonlinearity sets in at quite low field strengths, such that the potential drop of an elementary charge across a distance a, the radius, approximates k_BT. In other words, the field strength scales with the radius of the sphere instead of the Debye length, as holds for the Wien effect in strong electrolyte solutions.[1] Presumably this change results from our choice of parameters $\kappa a > 1$ and would be reversed for $\kappa a < 1$.

Appendix A. Polynomial Basis Functions

The Legendre polynomials in $c = \cos\theta$ are the usual ones $P_0 = 1$, $P_1 = c$, ..., and satisfy

$$\int_{-1}^{1} P_n(c)P_m(c)\,dc = 2(2n + 1)^{-1}\delta_{m,n} \quad \text{(A1)}$$

The Gegenbauer polynomials G_n are required only for $n > 1$, and with that restriction they satisfy

$$\int_{-1}^{1} G_n(c)G_m(c)(1 - c^2)^{-1}\,dc = 2[n(n - 1)(2n - 1)]^{-1}\delta_{m,n} \quad \text{(A2)}$$

The sequence of G_n's starts with $G_0 = 1$, $G_1 = -c$, $G_2 = (1 - c^2)/2$. For $n > 1$ the G_n vanish at $c = \pm 1$, and for functions satisfying this same boundary condition the G_n provide a complete and orthogonal basis set. The G_n may be computed from their relation to the P_n,

$$G_n = (P_{n-2} - P_n)/(2n - 1) \quad \text{(A3)}$$

This same relation together with recursion relations for P_n' gives a useful identity

$$G_n' = -P_{n-1} \quad \text{(A4)}$$

Appendix B. Linear Oscillatory Flow

The asymptotic concentration, charge, and potential fields are developed here for linear oscillatory flow. For the most part in the equations are derived by dropping terms from those obtained in section V. However, the discussion of the asymptotic charge density in section V can be improved for linear flow. It is not necessary to worry about contributions to the charge density that are nonlinear in the $h_i(\mathbf{R})$, nor is it any problem to correct the electrical potential for a slowly decaying charge density.

The distinction in section V between the h_j and f_j functions need not be maintained in the linear problem. Equation 5.7 becomes

$$h_j^n(R) = 2\pi i^n \int_{-\infty}^{+\infty} h_n^{(1)}(kR)(\mathcal{P}_n\mathcal{N}_j/\mathcal{D})k^2\,dk \quad \text{(B1)}$$

The superscript n is retained to label the order of Legendre polynomial being considered, but only $n = 1$ is physically relevant. Likewise the source functions $T_i(\mathbf{k})$ have projections only on $P_1(\cos\theta)$. As in section V, only the case $I = 2$, that is, when two species of mobile ions are present, is considered in any detail. For large I one should either

automate the generation of polynomials or follow the eigenvalue methods of DeLacey and White.[6]

Equation 5.9 becomes

$$\mathcal{N}_j^n = \mathcal{P}_n\mathcal{N}_j = -[T_j^n(k^2 + i\omega\gamma_j') + \sum_i (z_iT_j^n - z_jT_i^n)Z_i](-ik)^n \quad \text{(B2)}$$

Equation 5.18 has been used to factor out the dependence of T_i on $\mathbf{k}$. The quantities γ_i' are defined by $\gamma_1' = \gamma_2$ and $\gamma_2' = \gamma_1$. Equation 5.11 becomes

$$\mathcal{D} = k^4 + Bk^2 + C \quad \text{(B3)}$$

where

$$B \equiv 1 + i\omega(\gamma_1 + \gamma_2) \quad \text{(B4)}$$

and

$$C \equiv i\omega(z_1Z_1\gamma_2 + z_2Z_2\gamma_1) - \omega^2\gamma_1\gamma_2 \quad \text{(B5)}$$

Since $\mathcal{D}(k)$ is quadratic in k^2, it may be factored into

$$\mathcal{D} = (k^2 + \lambda_1^2)(k^2 + \lambda_2^2) \quad \text{(B6)}$$

λ_1 and λ_2 are presumed to be defined such that $i\lambda_1$ and $i\lambda_2$ lie in the upper half of the complex plane. Then repetition of the contour integration in section V, this time retaining all roots, gives

$$h_j^n(R) = A_j^n(\lambda_1)g_n(\lambda_1R) - A_j^n(\lambda_2)g_n(\lambda_2R) \quad \text{(B7)}$$

where $A_j^n(\lambda)$ is defined by

$$A_j^n(\lambda) = (i\omega\gamma_j' - \lambda^2)T_j^n + \sum_i (z_iT_j^n - z_jT_i^n)Z_i \quad \text{(B8)}$$

As before, constants have been absorbed into the T_j^n, since they are simply parameters that have to be obtained numerically, to fit the inner boundary conditions.

The charge density h_n is given by

$$h^n = \sum Z_ih_i^n = A^n(\lambda_1)g_n(\lambda_1R) - A^n(\lambda_2)g_n(\lambda_2R) \quad \text{(B9)}$$

where

$$A^n(\lambda) \equiv \sum Z_jA_j^n = \sum Z_j(i\omega\gamma_j' - \lambda^2)T_j^n \quad \text{(B10)}$$

Since the $g_n(\lambda R)$ are eigenfunctions of $\mathcal{L}_n$, the solution of

$$\mathcal{L}_n\phi_h^n = -h^n \quad \text{(B11)}$$

is readily seen to be

$$\phi_h^n = -\lambda_1^{-2}A^n(\lambda_1)g_n(\lambda_1R_1) + \lambda_2^{-2}A^n(\lambda_2)g_n(\lambda_2R) \quad \text{(B12)}$$

This is the correction to the multipole expansion of $\phi^n(R)$ to be used in eq 5.25.

Appendix C. Modified Spherical Bessel Functions

Our functions $g_n(\lambda R)$ are related to the $K_{n+1/2}$ of ref 15 by

$$g_n(\lambda R) = \lambda^{n+1}(2/\pi\lambda R)^{1/2}K_{n+1/2}(\lambda R) \quad \text{(C1)}$$

The g_n are eigenfunctions of $\mathcal{L}_n$ and satisfy

$$\mathcal{L}_ng_n = \lambda^2g_n \quad \text{(C2)}$$

The sequence starts with

$$g_0 = R^{-1}e^{-\lambda R} \quad \text{(C3)}$$

$$g_1 = R^{-2}(1 + \lambda R)e^{-\lambda R} \quad \text{(C4)}$$

Higher members of the series are generated by the recursion relations

$$g_{n+1} = \lambda^2g_{n-1} + (2n + 1)R^{-1}g_n \quad \text{(C5)}$$

and

$$\partial g_n/\partial R = -[\lambda^2g_{n-1} + (n + 1)R^{-1}g_n] \quad \text{(C6)}$$

Appendix D. Transformations

The transformations of dependent variables for numerical integration are described here. The dependent variables associated with the deviations from equilibrium are $h_i^n(R)$, $s^n(R)$, $w^n(R)$, and $\phi^n(R)$. These are designated generically as $y(R)$ and the differential operators $\mathcal{L}_n$ and $\mathcal{N}_n$ by $\mathcal{M}$:

$$\mathcal{M}y = X(R) \quad \text{(D1)}$$

$$\mathcal{M} \equiv \frac{\partial^2}{\partial R^2} + X_1(R)\frac{\partial}{\partial R} + X_2(R) \quad \text{(D2)}$$

The homogeneous equation $\mathcal{M}y = 0$ has solutions $y_1(R)$ and $y_2(R)$. For the problems at hand these solutions are $y_1 = R^{-(n+1)}$ and $y_2 = R^n$ for the operator $\mathcal{L}_n$, and $y_1 = R^{1-n}$ and $y_2 = R^n$ for the operator $\mathcal{N}_n$.

Equations 6.3 and 6.4 lead to

$$Y_1' = -y_2X/W \quad \text{(D3)}$$

$$Y_1 = (yy_2' - y'y_2)/W \quad \text{(D4)}$$

$$Y_2' = y_1X/W \quad \text{(D5)}$$

$$Y_2 = -(yy_1' - y'y_1)/W \quad \text{(D6)}$$

where W is the Wronskian

$$W \equiv y_1y_2' - y_1'y_2 \quad \text{(D7)}$$

For each of the physical fields, eq D3 and D5 add a pair of first-order differential equations to the coupled set that has to be integrated numerically. Equations D4 and D6 give the boundary conditions on the Y's in terms of the known boundary conditions on y and y'. The source functions X are tabulated in section IV and depend nonlinearly on the fields as well as on R.

To prevent numerical overflow and underflow for large α and R, the Y's associated with $\mathcal{L}_n$ or $\mathcal{N}_n$ are further transformed by

$$B_1(R) \equiv \alpha^{-n}Y_1(R) \quad \text{(D8)}$$

$$B_2(R) \equiv \alpha^nY_2(R) \quad \text{(D9)}$$

The equation for $\psi^e(R)$ was transformed to one for a new function $Y(R)$, defined by

$$\psi^e(R) \propto Y(R)R^{-1}e^{-R} \quad \text{(D10)}$$

a proportionally constant being chosen for convenience and to avoid underflow. At large R the boundary condition is $Y'(R) = 0$.

References and Notes

(1) Harned, H. S.; Owen, B. B. "The Physical Chemistry of Electrolytic Solutions"; Reinhold: New York, 1950.
(2) Hogan, M.; Dattagupta, N.; Crothers, D. M. *Proc. Natl. Acad. Sci. U.S.A.* **1978**, *75*, 195.
(3) Overbeek, J. Th.; Wiersema, P. H. "Electrophoresis"; Bier, M., Ed.; Academic Press: New York, 1967; Vol. 2, Chapter 1.
(4) Fixman, M. *J. Chem. Phys.* **1980**, *72*, 5177.
(5) O'Brien, R. W.; White, L. R. *J. Chem. Soc., Faraday Trans. 2* **1978**, *74*, 1607.
(6) DeLacey, E. H. B.; White, L. R. *J. Chem. Soc., Faraday Trans. 2* **1981**, *77*, 2007.
(7) Fixman, M. *Macromolecules* **1980**, *13*, 711.
(8) Fixman, M. *J. Chem. Phys.* **1981**, *75*, 4040.
(9) Fixman, M.; Jagannathan, S. *J. Chem. Phys.* **1981**, *75*, 4048.
(10) Dukhin, S. S.; Derjaguin, B. V. "Surface and Colloid Science"; Matijevic, E., Ed.; Wiley: New York, 1974; Chapter 2.
(11) Hynes, J. T. *Annu. Rev. Phys. Chem.* **1977**, *28*, 301.

(12) Happel, J.; Brenner, H. "Low Reynolds Number Hydrodynamics"; Noordhoff: Leyden, 1973.
(13) Fixman, M. *J. Chem. Phys.* **1983**, *78*, 1483.
(14) Morse, P. M.; Feshbach, H. "Methods of Theoretical Physics"; McGraw-Hill: New York, 1953.
(15) Abramowitz, M.; Stegun, I. A. "Handbook of Mathematical Functions"; National Bureau of Standards: Washington, D.C., 1964.
(16) Hall, G.; Watt, J. M., Eds. "Modern Numerical Methods for Ordinary Differential Equations"; Oxford University Press: Oxford, 1976.
(17) Gladwell, I.; Sayers, D. K., Eds. "Computational Techniques for Ordinary Differential Equations"; Academic Press: New York, 1980.
(18) Dahlquist, G.; Bjorck, A. "Numerical Methods"; Prentice-Hall: Englewood Cliffs, NJ, 1974.

Luminescence Techniques in Polymer Colloids. 1. Energy-Transfer Studies in Nonaqueous Dispersions

Onder Pekcan,† Mitchell A. Winnik,* and Luke Egan

Lash Miller Laboratories, Department of Chemistry, and Erindale College, University of Toronto, Toronto, Ontario, Canada M5S 1A1

Melvin D. Croucher

Xerox Research Centre of Canada, 2480 Dunwin Drive, Mississauga, Ontario, Canada L5L 1J9. *Received June 17, 1982*

ABSTRACT: Nonaqueous dispersions (1–3-μm diameter) of a polymer colloid were prepared containing naphthalene (N) groups covalently attached to the poly(methyl methacrylate) (PMMA) core. Cilia of polyisobutylene grafted onto PMMA served as the steric barrier to stabilize the dispersions. Typical naphthalene fluorescence was observed when isooctane suspensions of these colloids were irradiated at 280 nm. When anthracene (A) was added to the solvent, energy transfer $N^* + A \rightarrow N + A^*$ was observed. The rate constant for this process was 70 times slower than for the corresponding reaction between excited 1-naphthylmethyl pivalate and anthracene. These results are interpreted in terms of a diffusion model in which both anthracene diffusion and exciton diffusion play a role.

This paper describes results on the use of fluorescent labels to study the properties of nonaqueous dispersions of polymer colloids. Fluorescence techniques have seen wide applicability in biochemistry as tools to study the molecular morphology and molecular dynamics of complex systems.[1] More recently, these techniques have been applied to polymers. Several reviews on the subject have appeared.[2] Among the topics in polymer science studied by fluorescence techniques are molecular orientation and molecular motion in amorphous polymers,[2,3] chain interpenetration,[4] the thermodynamics of mixing in polymer blends,[5] and a wide spectrum of solution properties of polymers.[2,3] For example, our research group has developed a fluorescence technique for measuring the slowest internal (Rouse–Zimm) relaxation time of polymer chains in dilute and concentrated polymer solution.[6]

In this paper, we focus our attention on the fluorescence properties of polymer colloids[7a] that are sterically stabilized by cilia of polyisobutylene (PIB) and which contain naphthalene (N) groups covalently attached to the poly(methyl methacrylate) (PMMA) that comprises the core of the particle. These colloids form stable dispersions in alkane solvents and clear, homogeneous solutions in solvents such as chloroform and ethyl acetate, which can dissolve PMMA. We have examined the fluorescence of these dispersions in aliphatic alkanes, exciting the samples at 280 nm, where the N groups absorb. In subsequent experiments, we added anthracene (A) to the alkane dispersion medium for the colloid, since we wished to investigate the possibility that A might approach sufficiently close to the colloid's core surface to accept energy from a photoexcited N. Quenching of N* and sensitized A* fluorescence would result.

† On leave from the Department of Physics, Hacettepe University, Ankara, Turkey.

Scheme I

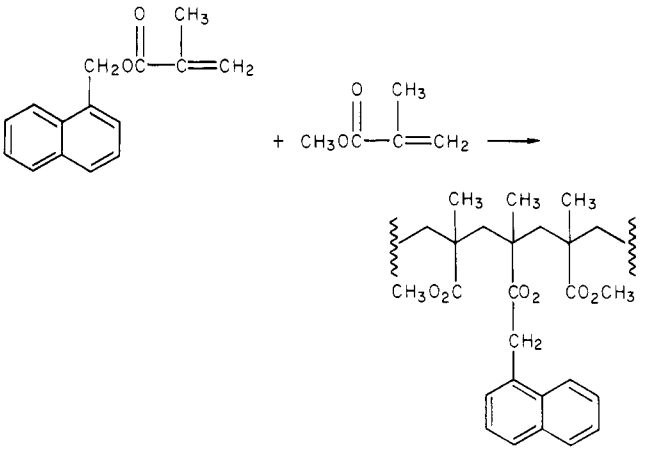

The PIB sterically stabilized PMMA colloids were prepared in a two-step procedure.[7b] In the first step, short PMMA sequences were grafted onto a PIB sample of nominal molecular weight 10^4. These PIB samples contain sites of unsaturation for reaction with either initiator radicals or growing PMMA chains. Polymerization is terminated before the PMA sequences become sufficiently long as to render the polymer insoluble in the cyclohexane reaction mixture. This short graft copolymer, called the "dispersant", is precipitated from solution with ethanol and purified.

In the second step of the preparation, the dispersant, methyl methacrylate (MMA), an initiator, and a methacrylate derivative of the desired chromophore are combined in cyclohexane solution and refluxed overnight. A white dispersion forms. The reaction is stopped before all the monomer is incorporated into the dispersion. This procedure produces spherical particles of relatively narrow distribution of sizes. Using 1-naphthylmethyl methacrylate

0024-9297/83/2216-0699$01.50/0